Acta Bot. Croat. 79 (2), 201–211, 2020
DOI: 10.37427/botcro-2020-026

CODEN: ABCRA 25
ISSN 0365-0588
eISSN 1847-8476

De novo transcriptome analysis of high growth rate *Pyropia yezoensis* (Bangiales, Rhodophyta) mutant with high utilization of nitrogen

Seo-jeong Park, Jong-il Choi*

Chonnam National University, Department of Biotechnology and Bioengineering, Interdisciplinary Program for Bioenergy and Biomaterials, Gwangju 61186, Republic of Korea

Abstract – *Pyropia yezoensis* (Ueda) M.S.Hwang et H.G.Choi (Bangiales, Rhodophyta) has potentially high economic value. *P. yezoensis* has been used as food in East Asian countries for a long time, and, in addition to that its consumption is increasing worldwide owing to the growing interest in healthy seaweed food. A mutant (Py2K) with a high growth rate was developed using gamma rays to increase the production of *P. yezoensis*. *De novo* transcriptome analysis was performed to determine the mechanism underlying the high growth rate of this mutant. The transcriptomes from wild-type (PyWT) and mutant (Py2K) strains were assembled, and 167,165 genes were analyzed. A total of 15,979 genes were differentially expressed. Transcriptome analysis of nitrogen pathway revealed the increase in nitrogen availability through the upregulation of nitrate transporter gene (*nrt*) expression. Activation of nitrogen assimilation and re-assimilation and upregulation in alternative oxidase (*aox*) gene contributed to the increase in cellular nitrogen availability, thereby affecting the synthesis of phycobiliprotein. As a consequence, the efficiency of photosynthesis and the subsequent growth rate increased, which contributed to the color differences in thalli between PyWT and Py2K.

Keywords: differentially expressed genes, high growth rate mutant, nitrogen availability, *Pyropia yezoensis*, RNA-sequencing, transcriptome analysis

Introduction

Seaweeds have been used as food and for medicines in East Asian countries for at least 1500 years (Hwang et al. 2019). The rhodophyte genus *Pyropia* J.Agardh (Bangiales) is a well-known farmed seaweed in East Asian countries such as Korea, Japan, and China. *Pyropia* is rich in nutrients including polysaccharides, proteins, steroids, carotenoids, long-chain poly-unsaturated fatty acids (PUFAs), and vitamins (Lee et al. 2016). The growing interest in seaweed-based food for the sake of health and nutrition (Van Loo et al. 2017) has increased the market demand for *Pyropia*, giving it a high potential economic value (Jiang et al. 2018). In addition to *Pyropia tenera* (Kjellman) N.Kikuchi, M.Miyata, M.S.Hwang et H.G.Choi, *P. seriata* (Kjellman) N.Kikuchi et M.Miyata, and *P. dentata* (Kjellman) N.Kikuchi et M.Miyata, *P. yezoensis* (Ueda) M.S.Hwang et H.G.Choi is one of the most cultivated species in Korea (Hwang et al. 2005).

Many studies have been directed an increasing the production of *Pyropia*, particularly through the control of algal diseases and using different cultivation technologies (Park et al. 2006, Kim et al. 2014, Kim et al. 2017). Selection, hybridization, and mutation are the basic methods used to develop seaweed strains suitable for mass cultivation, and nine *Pyropia* strains have been developed using these three methods in Korea from 2012 to 2018 (Park and Hwang 2014, Lee and Choi 2018, Hwang et al. 2019). Physical and chemical mutagens induce genetic variabilities in plants, and enhanced-tolerant mutants have been generated over the past 50 years (Beyaz and Yildiz 2017, Lee and Choi 2018). Several studies have also used mutagens to induce mutations in seaweed (Guimarães et al. 2003, Zayadan et al. 2014, Lee and Choi 2018). Gamma radiation is a physical mutagen generally used to obtain mutants with desirable traits. In this study, a mutant with high growth rate was developed using gamma rays. However, the mechanisms underlying its high growth rate were difficult to understand owing to the limited genetic information. Although some studies have published

* Corresponding author e-mail: choiji01@jnu.ac.kr

the draft and plastid genomes of *P. yezoensis*, information on its genome remains inadequate (Nakamura et al. 2013, Wang et al. 2013).

Transcriptome analysis using high-throughput RNA-sequencing (RNA-seq) offers the opportunity to investigate the molecular components *de novo*. Several transcriptome-based studies have been performed for non-model organisms such as seaweeds (Bryant et al. 2017, Carvalho et al. 2018, Garcia-Jimenez et al. 2018, Nan et al. 2018). The analysis of expressed transcripts may reveal unknown metabolic pathways or improve our knowledge about specific regulatory mechanisms.

In the present study, we performed *de novo* RNA-seq analysis to evaluate the mechanism underlying the high growth rate of the mutant *P. yezoensis*. Computational analysis of the transcriptome analysis result was combined with experiments to reveal the differences between the mutant and wild-type strains. This study aimed to elucidate the metabolic changes in the mutant strain with a high growth rate. The results of this study could improve our understanding about the functions of *Pyropia* genes and assist in the development of other mutants or recombinant seaweeds. Furthermore, the isolated mutant *Pyropia* with high growth will be useful in seaweed-based industries.

Materials and methods

Algal culture and development of a mutant with high growth rate

Pyropia yezoensis specimens were obtained from the Seaweed Research Center (Mokpo, Republic of Korea). Gametophytes of PyWT and Py2K were cultured in filter-sterilized Provasoli Enriched Seawater (PES) medium (Provasoli 1963) at 10 °C. A growth chamber set with a 10 h light and 14 h dark cycle (80 μmol photons·m^{-2}·s^{-1}) and filter-sterilized air was used. The medium was replaced every week.

Mutant *P. yezoensis* with a high growth rate was isolated as previously described (Lee and Choi 2019). Blades (1-2 cm long) were cultured for 4 weeks and exposed to ^{60}Co gamma rays at 2 kGy at a rate of 10 kGy h^{-1} (Nordion International, Ottawa, Ontario, Canada). The samples were allowed to recover at 10 °C for 24 h in the dark. The surviving cells were selected and cultivated under similar conditions for 30 days. The length and width of blades were measured every week, and blades longer and wider than wild-type blades were isolated. Isolated blades were cultured for 6 weeks under similar conditions. The selected mutant with high growth rate was termed as "Py2K."

RNA sequencing and *de novo* transcriptome analysis

The gametophytes were harvested after 4 weeks of cultivation and frozen in liquid nitrogen. Total RNA was prepared and sequenced by Insilicogen Company (Yongin, Republic of Korea) (Baek et al. 2018). The Illumina NextSeq 500 platform was used for pair-end RNA-seq.

Clean reads generated by Trimmomatic (Bolger et al. 2014) were assembled using Trinity (Haas et al. 2013) in an *in silico* normalization and a *de novo* assembly mode. The published draft genome of *P. yezoensis* (Nakamura et al. 2013) was used as the reference indexed with BBsplit in BBtools (Bushnell et al. 2017) to separate more reliable reads as *P. yezoensis* from clean reads. Putative contaminants were distinguished and eliminated from unmapped clean reads of *P. yezoensis* draft genome. Putative contaminants were distinguished using Diamond blast (Buchfink et al. 2015) with the NCBI non-redundant (NCBI-nr) database (Pruitt et al. 2005). The most annotated bacterial species were considered as putative contaminants. Mapped reads from *P. yezoensis* draft genome and unmapped reads from *P. yezoensis* and filter reads were merged and then *de novo* assembled using Trinity. The assemblies were separately generated from PyWT and Py2K.

The open-reading frame was identified by TransDecoder (Haas et al. 2013), and duplicates were eliminated using CD-HIT-EST (Li and Godzik 2006) by clustering based on at least 90% similarity. A shared sequence file between PyWT and Py2K was generated by CD-HIT-EST-2D and BBsplit. Transcriptome assembly was qualified using BUSCO v3 with Eukaryota database (Waterhouse et al. 2018).

Functional annotation and differential expressed genes (DEGs) analysis

NCBI-nr, SWISS-PROT (Consortium 2018), Pfam (Sonnhammer et al. 1997), and Kyoto Encyclopedia of Genes and Genomes (KEGG) (Kanehisa and Goto 2000) were used for annotation. TransDecoder was used to retrieve amino acid sequences, while BLASTp (Camacho et al. 2009) was employed to descript amino acid sequences from SWISS-PROT. DIAMOND (Buchfink et al. 2015) was used with NCBI-nr to annotate amino acid sequences, while conserved protein domains from Pfam were annotated with hmmscan (Finn et al. 2011). Functional annotation was processed with an e-value $\leq 1 \times 10^{-5}$. GO terms were annotated using the top BLASTp matched with sequences in SWISS-PROT as per the Trinotate workflow.

Gene abundance in sequences from PyWT and Py2K was estimated using Salmon (Patro et al. 2017). We used DEseq2 (Love et al. 2014) to identify DEGs between PyWT and Py2K at a false discovery rate (FDR) significant at ≤ 0.05 and an absolute value of $\log_2$ ratio ≥ 1. WEGO v2 was used to analyze functional interpretation (Ye et al. 2018).

Real-time quantitative polymerase chain reaction (RT-qPCR) was performed to validate the findings of transcriptome analysis using TB Green™ Premix Ex Taq™ (Tli RNaseH Plus, TaKaRa) on an Illumina Eco Real-Time system. All reactions were conducted in triplicate. *PyGADPH* was used as an internal control (Kong et al. 2015). The primer sets specific for selected unigenes were designed using Primer3 (Untergasser, et al. 2012) (On-line Suppl. Tab. 1).

Differential expression level was calculated by the $2^{(-\Delta\Delta Ct)}$ method (Livak and Schmittgen 2001), while relative expression was described by $\log_2 2^{(-\Delta\Delta Ct)}$. All experiments were performed in triplicate.

Antioxidant activity and polyphenol content

The 1,1-diphenyl-2-picryl-hydrazyl (DPPH) assay was performed as described by Jao and Ko (2002) and Nguyen et al. (2018). Harvested algal samples were powdered in liquid nitrogen using a mortar. Each ground sample (100 mg) was mixed with 80% ethanol at a ratio of 1:10 (w/v) and shaken at 100 rpm at 75 °C for 1 day. The mixture was filtered and condensed, and condensed samples were diluted with dimethyl sulfoxide (DMSO) to 20 mg mL^{-1}. Then, 100 µL DPPH (1.5×10^{-4} M) and a 100 µL sample (500 µg mL^{-1}) were placed in a 96-well plate, mixed, and reacted at 25 °C for 30 min. Absorbance was measured at 517 nm wavelength using a microplate reader (Molecular Devices, CA, San Jose, USA). The ferric ion-reducing antioxidant potential (FRAP) assay was performed with a ferric-reducing antioxidant power (FRAP) assay kit (Sigma-Aldrich, St. Louis, MO, USA) following the manufacturer's protocol.

Total polyphenolic content was measured as described by Maksimović et al. (2005). Ground algal samples and 80% acetone were mixed at a ratio of 1:100 (w/v) and incubated in a water bath at 20 °C for 6 h. The samples were centrifuged, and the supernatants obtained were incubated with Folin-Ciocalteu reagent (Sigma) at a ratio of 1:2 (v/v) at room temperature for 1 h. The absorbance of the reaction solution was measured at 750 nm wavelength using a microplate reader.

Determination of chlorophyll fluorescence and photosynthetic pigment content

The photochemical efficiency of the photosystem II (PSII; Fv/Fm) was determined for PyWT and Py2K using a microscopy pulse-amplitude modulation apparatus (Walz GmbH, Effeltrich, Germany) as previously described by Kim et al. (2006).

Phycoerythrin (PE) and phycocyanin (PC) levels were quantitatively analyzed as per the method described by Sampath-Wiley and Neefus (2007). Algal samples were ground in liquid nitrogen using a mortar, and 100 mg of powdered samples were incubated with 800 µL of 0.1 M phosphate buffer (pH 6.8) at 4 °C for 12 h. The incubated samples were centrifuged at 15,000 ×*g* for 10 min at 4 °C, and the supernatants obtained were mixed with 200 µL phosphate buffer by vortexing. Their absorbance was measured using a microplate reader at 564, 618, and 730 nm (Molecular Devices).

Chlorophyll *a* (Chl *a*) was extracted by incubating 100 mg powdered samples with 1.8 mL of 98% acetone for 2 h at 4 °C in the dark. The supernatants obtained after centrifugation at 5000 ×*g* for 10 min were used to determine spectrophotometrically the content of Chl *a*, as described by Jeffrey and Humphrey (1975). The mean of triplicate ± standard deviation was presented, and the Student *t*-test was used to determine the significance of the difference between the wild type and the mutant.

Results

De novo assembly and functional annotation of mutant *P. yezoensis* transcriptome

After exposure to 2 kGy gamma irradiation, a mutant of *P. yezoensis* with long and wide blades was isolated (Fig. 1A, B). The blades of Py2K were six times longer and three times wider than those of PyWT after 6 weeks of cultivation under similar conditions (Fig. 1C, D). Random amplified polymorphic DNA (RAPD) analysis was conducted to compare genotypic differences between PyWT and Py2K (Al-Zahim et al. 1999). Seven primer sets revealed the different patterns of amplified bands (On-line Suppl. Fig. 1), indicating that the isolated mutant was genetically distinct from the wild-type strain.

RNA was prepared from six samples, and approximately 424 million reads (151 base pairs) were generated by RNA-seq (On-line Suppl. Tab. 2). Elimination of putative contaminating sequences from the transcriptome yielded 197,780 transcripts and 167,165 genes (Tab. 1); N50 contained 672 bp and N10 contained 1,629 bp. While N50 was not long, N10 had sufficient length. The GC content was 52.42%, which was lower than the known GC content of the *P. yezoensis* genome. The E90 transcript set, indicative of the top 90% expressed transcripts, was 15,299 and the E90N50 was 675 bp. Thus, the assembled transcriptome contained near-complete gene sequence information for 78.2% genes in Eukaryota database (C: 78.2% [S: 43.9%, D: 34.3%], F: 16.5%, M: 5.3%, n: 303; C, complete BUSCOs; S, complete and single-copy BUSCOs; D, complete and duplicated BUSCOs; F, fragmented BUSCOs; M, missing BUSCOs; n, total BUSCO groups searched).

Genes were mostly annotated in NCBI-nr (140,721 genes; 71.65%), followed by Pfam (103,827 genes; 52.86%), GO (98,361 genes; 50.07%), SWISS-PROT (94,390 genes; 48.06%), and KEGG (82,023 genes; 41.76%). In total, 146,654 genes (74.67%) were annotated from at least one database.

DEGs from the wild-type and mutant variants and GO enrichment

We confirmed the high similarity between the heatmaps of samples from each group using Pearson's correlation coefficients (On-line Suppl. Fig. 2). In all, 15,979 genes were retained at an FDR ≤ 0.05 and absolute value of log2 ratio ≥ 1 (Fig. 2). In Py2K, 9,113 genes were upregulated and 6,866 genes were downregulated as compared to PyWT. A total of 14,658 DEGs (91.73%) were annotated in at least one database, and most DEGs were annotated in NCBI-nr (14,494

Tab. 1. Statistics of the assembled transcriptome of *Pyropia yezoensis* wild-type (PyWT) and mutant variant (Py2K) before and after the removal of putative contaminant sequences using BBtools.

Statistic	Shared sequences (PyWT and Py2K)	
	Before	After
Total trinity genes	170,461	167,165
Total trinity transcripts	202,789	197,780
GC (%)	52.58	52.42
Contig N10	1,623	1,629
Contig N50	675	672
Median contig length	495	492
Average contig	626.14	624.81
Total assembled bases	126,974,556	123,574,254

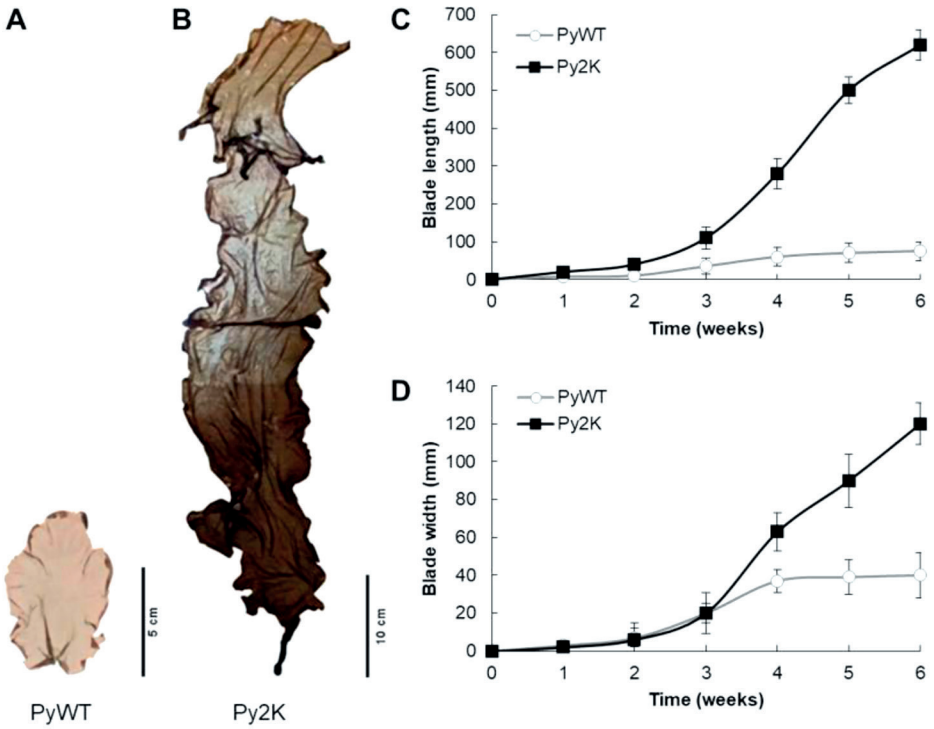

Fig. 1. *Pyropia yezoensis* wild-type (PyWT) and high growth rate mutant (Py2K). A – phenotype of PyWT, B – phenotype of Py2K cultivated for 6 weeks, C – growth of PyWT, D – growth of Py2K during 6 weeks of cultivation. Values are means ± standard deviation (n = 10).

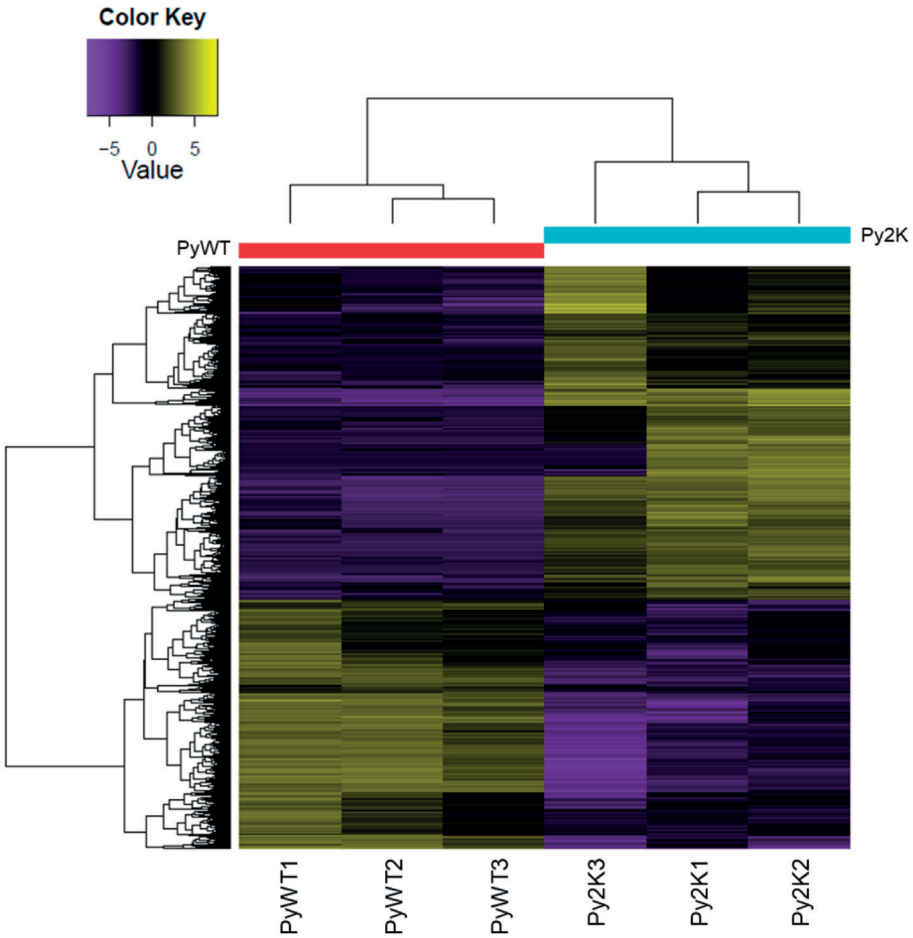

Fig. 2. Heatmap of differentially expressed genes (DEGs) between *Pyropia yezoensis* wild-type (PyWT) and mutant variants (Py2K). Each sample is on the x-axis and genes are on the y-axis. Purple and olive indicate downregulated and upregulated genes in the mutant, respectively.

Tab. 2. The photochemical efficiency of the photosystem II (Fv/Fm values) and chlorophyll *a* (Chl *a*), phycoerythrin (PE), and phycocyanin (PC) content in *Pyropia yezoensis* wild-type (PyWT) and mutant variant (Py2K). Mean of triplicate ± standard deviation is presented. Asterisk means the significant difference between PyWT and Py2K by the Student *t*-test (*P < 0.05, **P < 0.001).

Photochemical efficiency	PyWT	Py2K
Fv/Fm	0.58 ± 0.07	0.62 ± 0.08
Chl *a*	27.60 ± 0.54	28.54 ± 0.61
PE	175.12 ± 2.54	180.33 ± 1.76*
PC	180.33 ± 2.61	241.48 ± 2.51**
PE/Chl *a*	6.34 ± 1.43	6.33 ± 0.82
PC/Chl *a*	6.53 ± 1.49	8.47 ± 1.35*
PE + PC/Chl *a*	12.88 ± 1.19	14.8 ± 0.96*

DEGs; 90.70%), followed by Pfam (10,703 DEGs; 66.98%), GO (9,531 DEGs; 59.65%), SWISS-PROT (9,251 DEGs; 57.89%), and KEGG (8,042 DEGs; 50.33%).

GO term enrichment analysis revealed the annotation of 17 GO terms (Fig. 3). Four of these GO terms were mostly annotated in cellular process (GO:0009987, Biological Process), catalytic activity (GO:0003824, Molecular Function), cell (GO:0005623, Cellular Component), and cell part (GO:0044464, Cellular Component).

RT-qPCR was conducted to validate the results of transcriptome analysis with 10 randomly selected DEGs. Most genes showed similar expression patterns with DEGs (Online Suppl. Fig. 3). Thus, RT-qPCR analysis confirmed the validity of the transcriptome analysis.

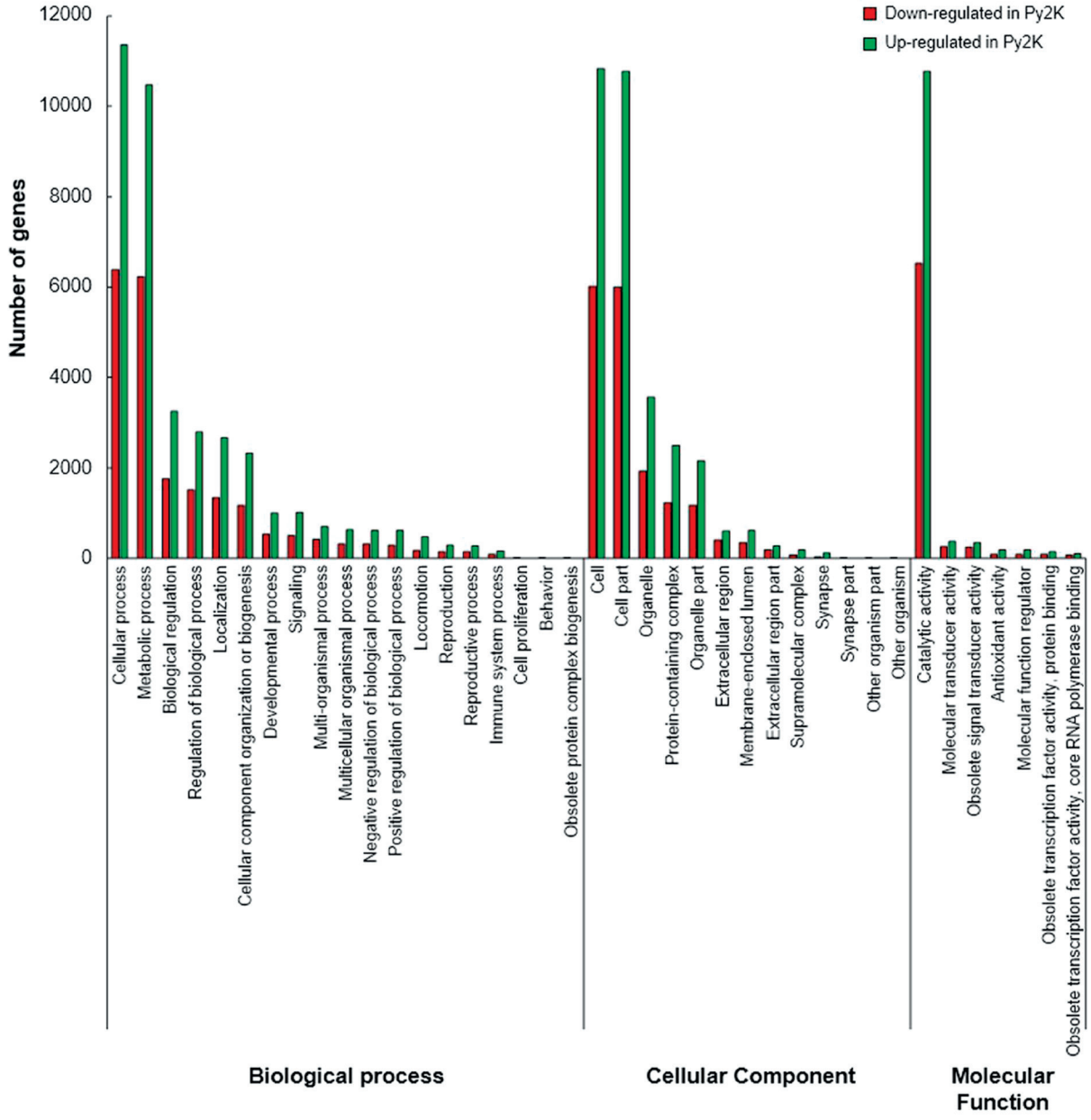

Fig. 3. Distribution of genes ontology terms in differentially expressed genes in *Pyropia yezoensis* wild-type and mutant variant (Py2K).

Upregulated transcripts in the mutant strain

The transcripts that were overexpressed in Py2K were related to antioxidant enzymes, shikimate pathway, nitrogen utilization, ribosome biogenesis, and energy generation. Antioxidant enzymes such as glutathione peroxidase, glutathione S-transferase, glutathione synthetase, peroxiredoxin, catalase, thioredoxin, and aldehyde dehydrogenase were found to be upregulated in the mutant strain (On-line Suppl. Tab. 3). The expression of some genes (chorismite synthase [*cs*], 3-dehydroquinate dehydratase [*DHQase*], shikimate kinase [*sk*], and shikimate dehydrogenase [*sdh*]), including those involved in the shikimate pathway related to phenol precursors, was upregulated in the mutant (On-line Suppl. Tab. 4, On-line Suppl. Fig. 4). Various transcripts related to the pathways utilizing nitrogen were overexpressed in Py2K (Fig. 4, On-line Suppl. Tab. 5). Moreover, the expression of various transcripts related to energy production such as the Calvin cycle, electron transport chain (ETC), and photosynthesis also increased in Py2K as follows: mitochondrial complex I, II, III, IV, V (genes encoding NADH-ubiquinone oxidoreductase, succinate dehydrogenase, CoQ-cytochrome c reductase, cytochrome c oxidase, and F_1F_0 ATP synthase, respectively), cytochrome c (Cyt c), isocitrate dehydrogenase (*idh*), and heme oxygenase (*ho*) (Fig. 4, On-line Suppl. Tab. 6).

Increased antioxidant capacity and content of photosynthetic pigments in the mutant strain

DPPH and FRAP assays were performed to confirm the increase in the antioxidant capacity of Py2K (Fig. 5A, B). DPPH radical-scavenging activity of Py2K was higher

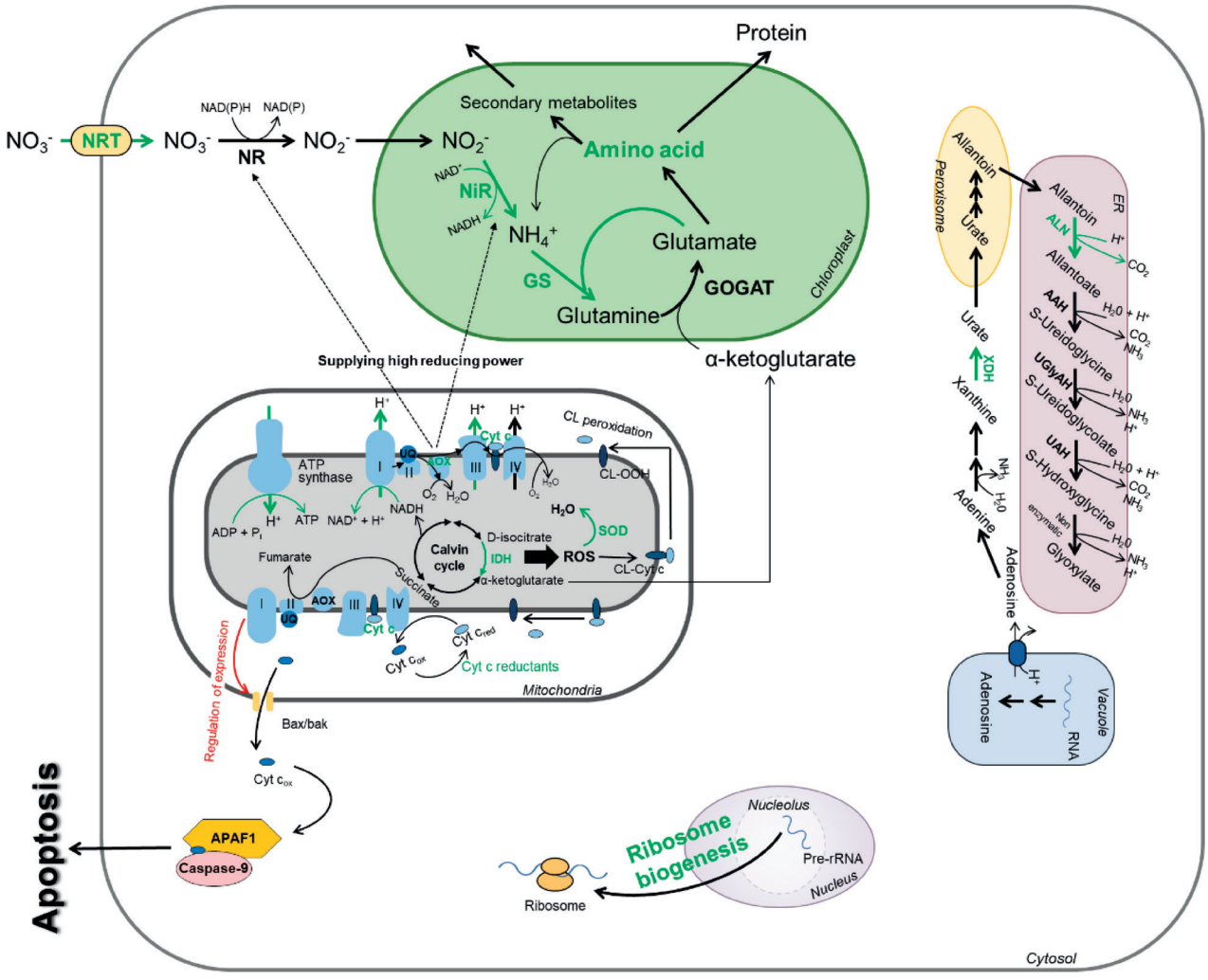

Fig. 4. Description of differentially expressed genes (DEGs) related to the high growth rate of the *Pyropia yezoensis* mutant Py2K. Nitrogen assimilation pathway is shown as described by Lillo (2004). The green and red arrows indicate upregulated and downregulated genes in Py2K– respectively. Abbreviations: NRT – nitrate transporter, NR – nitrate reductase, Nir – ferredoxin-nitrite reductase, GS – glutamine synthetase, GOGAT – glutamine oxoglutarate aminotransferase, XDH – xanthine dehydrogenase, ALN – allantoinase (allantoin amidohydrolase), AAH – allantoate amidohydrolase, UGlyAH – ureidoglycine aminohydrolase, UAH – ureidoglycolate amidohydrolase, ER – endoplasmic reticulum, CL – cardiolipin, mitochondrial complex: I – NADH dehydrogenase, complex II – succinate dehydrogenase, complex III – cytochrome c oxidase, complex IV – cytochrome c oxidase, UQ – ubiquinone, Cyt c – cytochrome c, Cyt c_{ox} – oxidized cytochrome c, Cyt c_{red} – reduced cytochrome c, AOX – alternative oxidase, IDH – isocitrate dehydrogenase, APAF1 – apoptotic protease-activating factor 1.

(78.43%) than that of PyWT (69.80%), while FRAP assay revealed a higher level of Fe^{3+} in Py2K (408.80 nM) than in PyWT (237.06 nM). We analyzed total phenolic content and found that the phenol content of Py2K was higher than that of PyWT (Fig. 5C).

The Fv/Tm value of Py2K was higher than that of PyWT, while Py2K contained more PE and PC than PyWT (Tab. 2). However, the content of Chl *a* slightly increased in Py2K over that in PyWT.

Discussion

In this study, a mutant *P. yezoensis* strain with high growth rate, Py2K, was obtained by gamma irradiation. Transcriptome analysis was performed *de novo* to elucidate differences in phenotypes between mutant Py2K and wild-type strains.

Transcriptome analysis revealed the upregulation in the expression of antioxidant enzymes in the mutant Py2K variant. Normal cellular metabolism generates reactive oxygen species (ROS) as a byproduct (Poljsak et al. 2013). High growth rate may induce the generation of excessive ROS as compared with normal growth conditions, owing to the activation of cellular metabolism. ROS could damage cells and, hence, antioxidants play an important role as scavengers of excessively produced ROS to limit ROS-induced damage. The increase in the antioxidant capacity of mutants developed with gamma rays is common and related to the mechanisms by which mutation is induced, involving generation of ROS or free radicals in cells (Beyaz and Yildiz 2017). The results of DPPH and FRAP assays show that Py2K had higher antioxidant capacity than did PyWT. The FRAP assay measures antioxidant capacity based on reducing power. Higher values in FRAP assay for mutant samples may indicate the additional components of Py2K as sources of reducing power. The content of total phenolic compounds, which act as reducing agents donating a single electron or hydrogen atom (Rabeta and Faraniza 2013), was higher in mutant Py2K than in the wild-type strain. Further, transcriptome analysis showed the activation of the biosynthesis pathway for phenol precursor, probably owing to the increase in the content of phenolics in the mutant strain. Therefore, high expression of antioxidant enzymes and increased levels of phenolic compounds could enhance the ROS-scavenging capacity of mutant Py2K.

The high growth of Py2K could be associated with the increased availability of nitrogen and energy regeneration system. Nitrogen is an essential nutrient and a limiting macronutrient in the ocean (Moore et al. 2013, Bristow et al. 2017). Nitrogen is assimilated in the following manner: NO_3^- uptake → NO_3^- → NO_2^- → NH_4^+ → glutamine → glutamate → amino acids (Lillo 2004). The gene *nrt* encodes a transporter that is located in the cell membrane and is involved in nitrate uptake. There are two forms of these genes, *nrt1* and *nrt2*. In general, the members of the *nrt1* family have low affinity for nitrate, while those of the *nrt2* family exhibit high affinity for nitrate (Lillo 2004). In the transcriptome analysis, we failed to observe *nrt1* as a DEG; however, *nrt2* expression was upregulated in Py2K (On-line Suppl. Tab. 5). Assimilated NO_3^- is reduced to NH_4^+ by NR and NiR. The expression of *nir* is induced by nitrate, which is generated by NR. NH_4^+ is used to produce glutamine via glutamine synthetase (*gs*) in the chloroplast, and glutamine is converted to glutamate, which is used for amino acid synthesis. The expression of *gs* and the genes related to amino acid synthesis (those encoding D-amino-acid N-acetyltransferase, cystathionine gamma-lyase, and arginosuccinate synthase) was upregulated in Py2K. NO_3^- uptake could be enhanced following increased

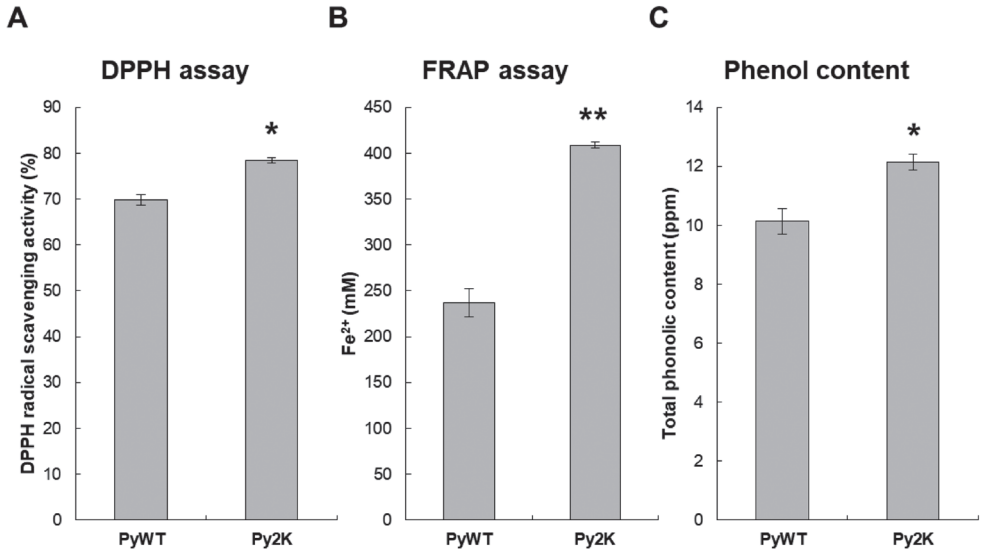

Fig. 5. Antioxidant capacity of *Pyropia yezoensis* wild-type (PyWT) and mutant variant (Py2K) determined using: A – 1,1-diphenyl-2-picryl-hydrazyl (DPPH) assay, B – ferric ion-reducing antioxidant potential (FRAP) assay, C – total phenolic content. Values are means ± standard deviation (n = 3). The Student *t*-test was conducted to define the difference between PyWT and Py2K. Asterisk means the significant difference between PyWT and Py2K by the Student *t*-test (*P < 0.05, **P < 0.001).

nrt expression, which resulted in increased synthesis of amino acids that were used as building blocks.

Nucleobases are rich stores of nitrogen in cells (Werner et al. 2013). Purine degradation results in the release of nitrogen, which is re-assimilated into amino acids. Purine ring catabolism via ureide-degrading reactions generates five NH_3 molecules from one adenosine molecule. The purine ring catabolism pathway was constructed using ureide-degrading reactions with reference to Werner and Witte (2011), Hafez et al. (2017) and, Melino et al. (2018), although this pathway is controversial in plants. The genes *aln* and *aah* (encoding allantoate amidohydrolase) are important for purine ring catabolism, and *Arabidopsis* mutants deficient in *aln* and *aah* had accelerated senescence, rapid transition, and impairment in reproductive growth (Takagi et al. 2018) (Fig. 4). Upregulated expression of *aln* could contribute to the activation of purine ring catabolism, and activated nitrogen re-assimilation would allow mutant variants to grow at higher rates than the wild-type strain.

Ribosome biogenesis is an important process regulating plant growth and development (Hang et al. 2018). Repressed ribosome biogenesis results in defective vegetable growth and development (Beine-Golovchuk et al. 2018, Maekawa and Yanagisawa 2018, Palm et al. 2019). Repression of ribosome biogenesis is imperative under starvation conditions because it is one of the most energy consuming cellular processes (Kraft et al. 2008, Ohbayashi and Sugiyama 2018). However, transcripts related to ribosome biogenesis were upregulated in Py2K (On-line Suppl. Tab. 5), indicating that their high growth rate may induce the underutilization of cellular nitrogen as building blocks and mediate activation of nitrogen assimilation and re-assimilation; ribosome biogenesis replenished the cellular building blocks that were lacking.

Oxidative phosphorylation generates the bulk of ATP from mitochondria that is essential for the maintenance and growth of cells (Millar et al. 2011). In plants, the electron transport chain (ETC) comprises the mitochondrial complex I, II, III, IV, and V, ubiquinone (UQ), Cyt c, and alternative oxidase (AOX). Enhanced ETC leads to the generation of higher ATP levels, which subsequently support cell maintenance. Cyt c, a small heme protein and an essential component of the ETC in mitochondria, was found to be upregulated in Py2K (Virolainen et al. 2002, Ott et al. 2002, Reape et al. 2008, Matsuura et al. 2016). The presence of bax/bak in the outer membrane and peroxidation of cardiolipin (CL) stimulate the release of Cyt c. The expression of bax/bak is negatively regulated by the mitochondrial complex I (Kim et al. 2003, Westphal et al. 2011). Upregulated expression of mitochondrial complex I may result in the repression of the expression of bax/bak in the mutant variant. Further, CL peroxidation can be induced by ROS generated from oxidative phosphorylation to produce CL hydroperoxide (CL-OOH) and free Cyt c (Perier et al. 2005, de Paepe et al. 2014). Released Cyt c is immediately oxidized to Cyt c_{ox}, which activates caspase and combines with caspase-9 and apoptotic protease activating factor 1 (APAF1) to form a complex that promotes apoptosis (McMillin and Dowhan 2002, Vianello et al. 2007, Brown and Borutaite 2008).

Py2K showed upregulated expression of mitochondrial manganese-dependent superoxide dismutase (*mnsod*), which removes ROS generated from activated ETC (Vanlerberghe 2013) and prevents ROS-mediated CL peroxidation and the release of Cyt c. Cyt c reductants can reduce Cyt c_{ox} to Cyt c_{red} (Brown and Borutaite 2008) and may include superoxide, ascorbate, reduced glutathione, cytochrome P450, cytochrome b5, NAD(P)H, and tetramethyl-p-phenylenediamine.

In general, plant mitochondria contain AOX in their ETC systems (Vanlerberghe 2013). AOX is located between mitochondrial complexes II and III, and electrons are distributed to AOX and complex III. AOX is a non-proton pumping oxidase that can reduce the production of ROS generated from complex I and III. In addition, the expression of *aox* gene is upregulated under abiotic/biotic stress conditions because increased AOX expression is beneficial for maintaining homeostasis and to increase resistance against stress. AOX contributes to redox homeostasis for nitrate assimilation by supplying high reducing power to reduce nitrate to NH_4^+ (Vanlerberghe 2013). Stress conditions such as deficient cellular nitrogen may upregulate the expression of *aox* and contribute to nitrate assimilation by supplying high reducing power.

The Calvin cycle provides organic acids, and the ETC oxidizes NADH. The increase in the expression of *idh* may result in the activation of the Calvin cycle in Py2K mutant and contribute to ETC activation. Therefore, these findings suggest the activation of oxidative phosphorylation in the high growth rate mutant. Upregulated Cyt c expression could induce apoptosis; however, the high level of cytochrome b5 in Py2K may be useful to reduce oxidized Cyt c; thus, Cyt c may not induce apoptosis. Furthermore, the increased expression of *aox* could provide high reducing power for nitrate assimilation and prevent excessive ROS production (Fig. 4, On-line Suppl. Tab. 6).

Photosynthesis is the process in which energy is derived from light and stored in the form of nutrients. *P. yezoensis* uses Chl *a* and phycobiliproteins to obtain light for photosynthesis. Photosynthesis efficiency determines the growth of *P. yezoensis*, and an increase in photosynthesis efficiency may enhance the growth of *P. yezoensis* (Gao et al. 1991). Although Chl *a* is a photosynthetic pigment in plants and algae, the high phycobiliprotein content and phycobiliprotein/Chl *a* ratio indicate enhanced energy efficiency and rapid growth (Zhang et al. 2014). The increased Fv/Tm value and PE + PC/Chl *a* ratio in Py2K suggest that the enhanced photosynthetic efficiency may contribute to the high growth rate of the mutant (Tab. 2).

In summary, DEGs analysis revealed the increase in nitrogen uptake owing to the upregulated expression of *nrt* and that the activation of nitrogen assimilation and re-assimilation may serve as reasons for the high growth rate of the mutant (Fig. 6). In addition, *aox* expression was upregulated in

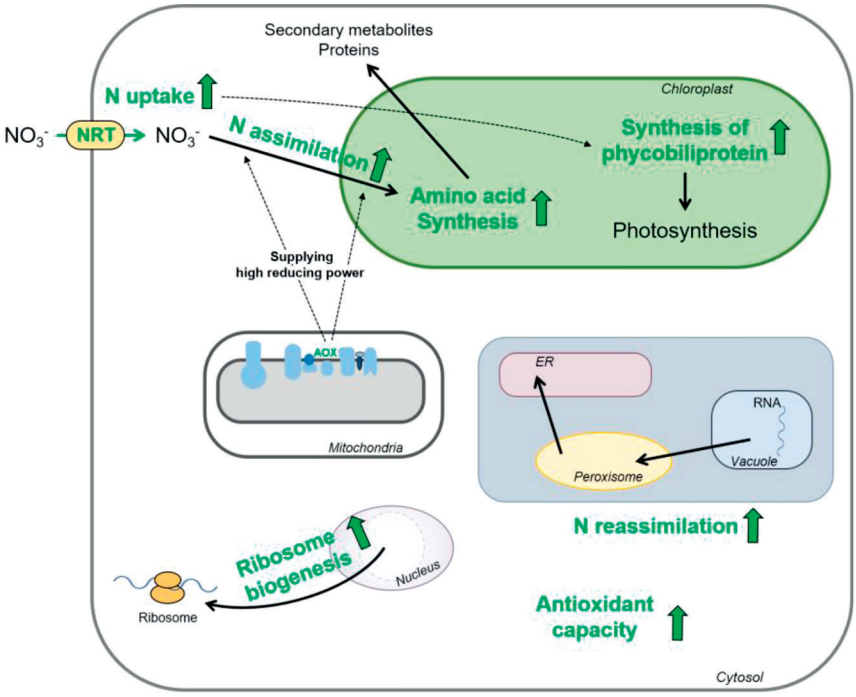

Fig. 6. Transcriptomic analysis for *Pyropia yezoensis* mutant. The green arrows indicate activated pathways related to the high growth rate of the mutant. AOX – alternative oxidase, N – nitrogen, NRT – nitrate transporter, ER – endoplasmic reticulum.

mitochondria and may have led to nitrogen assimilation by supplying NAD(P)H (Vanlerberghe 2013). Nitrogen availability might have increased and enhanced amino acid synthesis and ribosome biogenesis. Increased contents of amino acids as building blocks and high number of ribosomes could be useful during cell growth. Furthermore, increased nitrogen availability may regulate the synthesis of photosynthetic pigments and generate high levels of PE and PC in Py2K (Gao et al. 2019). The high expression of the genes related to the synthesis of phycobiliprotein precursor was evident in DEG analysis. High levels of PE and PC could enhance photosynthesis in the mutant, thereby increasing its growth rate (Zhang et al. 2014). Further, the differences in the levels of PE and PC between the mutant and PyWT may have led to variations in algal color (Fig. 1A, B). Increased nitrogen availability may activate cellular processes such as photosynthesis and induce the production of ROS. Some genes related to antioxidants were highly expressed in Py2K. Improved antioxidant capability may sufficiently scavenge ROS during the activation of cellular processes and prevent cell death.

In this study, transcriptome analysis was performed to understand the metabolic changes in the newly isolated mutant *Pyropia* Py2K. Py2K has a high growth rate and would be useful in seaweed cultivation. Furthermore, the transcriptome analysis performed could be useful for an understanding of the expression pattern of genes and the development of new cultivars of seaweeds for which genetic information is missing.

Acknowledgements

This work was supported by the National Research Foundation of Korea (NRF) grant funded by the Korea government (MSIT) (NRF-2018R1D1A1B07049359) and a Golden Seed Project Grant funded by Ministry of Oceans and Fisheries (213008-05-4-SB910).

References

Al-Zahim, M., Ford-Lloyd, B., Newbury, H., 1999: Detection of somaclonal variation in garlic (*Allium sativum* L.) using RAPD and cytological analysis. Plant Cell Reports 6, 473–477.

Baek, S.J., Chun, J.M., Kang, T.W., Seo, Y.S., Kim, S.B., Seong, B., Jang, Y., Shin, G.H., Kim, C., 2018: Identification of epigenetic mechanisms involved in the anti-asthmatic effects of *Descurainia sophia* seed extract based on a multi-omics approach. Molecules 23, 2879.

Beine-Golovchuk, O., Firmino, A.A.P., Dąbrowska, A., Schmidt, S., Erban, A., Walther, D., Zuther, E., Hincha, D.K., Kopka, J., 2018: Plant temperature acclimation and growth rely on cytosolic ribosome biogenesis factor homologs. Plant Physiology 176, 2251–2276.

Beyaz, R., Yildiz, M., 2017: The use of gamma irradiation in plant mutation breeding. In: Jurić, S. (ed.) Plant Engineering, 34–46. IntechOpen, London.

Bolger, A.M., Lohse, M., Usadel, B., 2014: Trimmomatic: a flexible trimmer for Illumina sequence data. Bioinformatics 30, 2114–2120.

Bristow, L.A., Mohr, W., Ahmerkamp, S., Kuypers, M.M., 2017: Nutrients that limit growth in the ocean. Current Biology 27, R474–R478.

Brown, G.C., Borutaite, V., 2008: Regulation of apoptosis by the redox state of cytochrome c. Biochimica et Biophysica Acta 1777, 877–881.

Bryant, D.M., Johnson, K., DiTommaso, T., Tickle, T., Couger, M.B., Payzin-Dogru, D., Lee, T.J., Leigh, N.D., Kuo T.H., Davis, F.G., 2017: A tissue-mapped axolotl *de novo* transcriptome enables identification of limb regeneration factors. Cell Reports 18, 762–776.

Buchfink, B., Xie, C., Huson, D.H., 2015: Fast and sensitive protein alignment using DIAMOND. Nature Methods 12, 59.

Bushnell, B., Rood, J., Singer, E., 2017: BBMerge–accurate paired shotgun read merging via overlap. PLoS One 12, e0185056.

Camacho, C., Coulouris, G., Avagyan, V., Ma, N., Papadopoulos, J., Bealer, K., Madden, T. L., 2009: BLAST+: architecture and applications. BMC Bioinformatics 10, 421.

Carvalho, E.L., Maciel, L.F., Macedo, P.E., Dezordi, F.Z., Abreu, M.E., Victória, F.d.C., Pereira, A.B., Boldo, J.., Wallau, G.D.L., Pinto, P.M., 2018: *De novo* assembly and annotation of the Antarctic alga *Prasiola crispa* transcriptome. Frontiers in Molecular Biosciences 4, 89.

Consortium, U., 2018: UniProt: the universal protein knowledgebase. Nucleic Acids Research 46, 2699.

de Paepe, R., Lemaire, S.D., Danon, A., 2014: Cardiolipin at the heart of stress response across kingdoms. Plant Signaling and Behavior 9, e29228.

Finn, R.D., Clements, J., Eddy, S.R., 2011: HMMER web server: interactive sequence similarity searching. Nucleic Acids Research 39, W29–W37.

Gao, G., Gao, Q., Bao, M., Xu, J., Li, X., 2019: Nitrogen availability modulates the effects of ocean acidification on biomass yield and food quality of a marine crop *Pyropia yezoensis*. Food Chemistry 271, 623–629.

Gao, K., Aruga, Y., Asada, K., Ishihara, T., Akano, T., Kiyohara, M., 1991: Enhanced growth of the red alga *Porphyra yezoensis* Ueda in high CO_2 concentrations. Journal of Applied Phycology 4, 355–362.

Garcia-Jimenez, P., Llorens, C., Roig, F.J., Robaina, R.R., 2018: Analysis of the Transcriptome of the Red Seaweed *Grateloupia imbricata* with Emphasis on Reproductive Potential. Marine Drugs 16, 490.

Guimarães, M., Plastino, E.M., Destombe, C., 2003: Green mutant frequency in natural populations of *Gracilaria domingensis* (Gracilariales, Rhodophyta) from Brazil. European Journal of Phycology 2, 165–169.

Haas, B.J., Papanicolaou, A., Yassour, M., Grabherr, M., Blood, P.D., Bowden, J., Couger, M.B., Eccles, D., Li, B., Lieber, M., 2013: *De novo* transcript sequence reconstruction from RNA-seq using the Trinity platform for reference generation and analysis. Nature Protocols 8, 1494.

Hafez, R.M., Abdel-Rahman, T.M., Naguib, R.M., 2017: Uric acid in plants and microorganisms: Biological Applications and Genetics-A review. Journal of Advanced Research 8, 475–486.

Hang, R., Wang, Z., Deng, X., Liu, C., Yan, B., Yang, C., Song, X., Mo, B., Cao, X., 2018: Ribosomal RNA Biogenesis and Its Response to Chilling Stress in *Oryza sativa*. Plant Pphysiology 177, 381–397.

Hwang, E.K., Yotsukura, N., Pang, S.J., Su, L., Shan, T.F., 2019: Seaweed breeding programs and progress in eastern Asian countries. Phycologia 5, 484–495.

Hwang, M.S., Kim, S.M., Ha, D.S., Baek, J.M., Kim, H.S., Choi, H.G., 2005: DNA sequences and identification of *Porphyra* cultivated by natural seeding on the southwest coast of Korea. Algae 3, 183–196.

Jao, C.L., Ko, W.C., 2002: 1, 1-Diphenyl-2-picrylhydrazyl (DPPH) radical scavenging by protein hydrolyzates from tuna cooking juice. Fisheries Science 2, 430–435.

Jeffrey, S.T., Humphrey, G., 1975: New spectrophotometric equations for determining chlorophylls a, b, c1 and c2 in higher plants, algae and natural phytoplankton. Biochemie und Physiologie der Pflanzen 2, 191–194.

Jiang, H., Zou, D., Lou, W., Deng, Y., Zeng, X., 2018: Effects of seawater acidification and alkalization on the farmed seaweed, *Pyropia haitanensis* (Bangiales, Rhodophyta), grown under different irradiance conditions. Algal Research 31, 413–420.

Kanehisa, M., Goto, S., 2000: KEGG: kyoto encyclopedia of genes and genomes. Nucleic Acids Research 28, 27–30.

Kim, G.H., Moon, K.H., Kim, J.Y., Shim, J., Klochkova, T.A., 2014: A revaluation of algal diseases in Korean *Pyropia* (*Porphyra*) sea farms and their economic impact. Algae 4, 249.

Kim, J.K., Yarish, C., Hwang, E.K., Park, M., Kim, Y., 2017: Seaweed aquaculture: cultivation technologies, challenges and its ecosystem services. Algae 1, 1–13.

Kim, K.Y., Jeong, H.J., Main, H.P., Garbary, D.J., 2006: Fluorescence and photosynthetic competency in single eggs and embryos of *Ascophyllum nodosum* (Phaeophyceae). Phycologia 3, 331–336.

Kim, M., Ahn, J.W., Jin, U.H., Choi, D., Paek, K.H., Pai, H.S., 2003: Activation of the programmed cell death pathway by inhibition of proteasome function in plants. Journal of Biological Chemistry 278, 19406–19415.

Kong, F., Cao, M., Sun, P., Liu, W., Mao, Y., 2015: Selection of reference genes for gene expression normalization in *Pyropia yezoensis* using quantitative real-time PCR. Journal of Applied Phycology 2, 1003–1010.

Kraft, C., Deplazes, A., Sohrmann, M., Peter, M., 2008: Mature ribosomes are selectively degraded upon starvation by an autophagy pathway requiring the Ubp3p/Bre5p ubiquitin protease. Nature Cell Biology 10, 602.

Lee, H.J., Choi, J., 2018: Isolation and characterization of a high-growth-rate strain in *Pyropia yezoensis* induced by ethyl methane sulfonate. Journal of Applied Phycology 4, 2513–2522.

Lee, J.H., Kim, H.H., Ko J.Y., Jang J.H., Kim G.H., Lee J.S., Nah J.W., Jeon Y.J., 2016: Rapid preparation of functional polysaccharides from *Pyropia yezoensis* by microwave-assistant rapid enzyme digest system. Carbohydrate Polymers 153, 512–517.

Lee, H.J., Choi, J., 2019: Enhancing temperature tolerance of *Pyropia tenera* (Bangiales) by inducing mutation. Phycologia 5, 496-503.

Li, W., Godzik, A., 2006: Cd-hit: a fast program for clustering and comparing large sets of protein or nucleotide sequences. Bioinformatics 22, 1658–1659.

Lillo, C., 2004: Light regulation of nitrate uptake, assimilation and metabolism. In: Amâncio, S., Stulen, I. (eds.), Nitrogen acquisition and assimilation in higher plants, 149–184. Springer, Dordrecht.

Livak, K.J., Schmittgen, T.D., 2001: Analysis of relative gene expression data using real-time quantitative PCR and the 2–ΔΔCT method. Methods 25, 402–408.

Love, M.I., Huber, W., Anders, S., 2014: Moderated estimation of fold change and dispersion for RNA-seq data with DESeq2. Genome Biology 15, 550.

Maekawa, S., Yanagisawa, S., 2018: Nucleolar stress and sugar response in plants. Plant Signaling and Behavior 13, e1442975.

Maksimović, Z., Malenčić, Đ., Kovačević, N., 2005: Polyphenol contents and antioxidant activity of Maydis stigma extracts. Bioresource Technology 96, 873–877.

Matsuura, K., Canfield, K., Feng, W., Kurokawa, M., 2016: Metabolic regulation of apoptosis in cancer. In International Review of Cell and Molecular Biology 327, 43–87.

McMillin, J.B., Dowhan, W., 2002: Cardiolipin and apoptosis. Biochimica et Biophysica Acta 1585, 97–107.

Melino, V.J., Casartelli, A., George, J., Rupasinghe, T., Roessner, U., Okamoto, M., Heuer, S., 2018: RNA catabolites contribute to the nitrogen pool and support growth recovery of wheat. Frontiers in Plant Science 9, 1539.

Millar, A.H., Whelan, J., Soole, K.L., Day, D.A., 2011: Organization and regulation of mitochondrial respiration in plants. Annual Review of pPant Biology 62, 79–104.

Moore, C., Mills, M., Arrigo, K., Berman-Frank, I., Bopp, L., Boyd, P., Galbraith, E., Geider, R., Guieu, C., Jaccard, S., 2013: Processes and patterns of oceanic nutrient limitation. Nature Geoscience 9, 701.

Nakamura, Y., Sasaki, N., Kobayashi, M., Ojima, N., Yasuike, M., Shigenobu, Y., Satomi, M., Fukuma, Y., Shiwaku, K., Tsujimoto, A., 2013: The first symbiont-free genome sequence of marine red alga, Susabi-nori (*Pyropia yezoensis*). PLoS One 8, e57122.

Nan, F., Feng, J., Lv, J., Liu, Q., Xie, S., 2018: Transcriptome analysis of the typical freshwater rhodophytes *Sheathia arcuata* grown under different light intensities. PLoS One 13, e0197729.

Nguyen, T.T., Choi, Y.J., Nguyen, T.H.P., Neri, T.A., Choi, B.D., 2018: Change in the antioxidant activity of roasted seasoned laver *Pyropia yezoensis* with heat processing and storage. Korean Journal of Fisheries and Aquatic Sciences 4, 362–368.

Ohbayashi, I., Sugiyama, M., 2018: Plant nucleolar stress response, a new face in the NAC-dependent cellular stress responses. Frontiers in Plant Science 8, 2247.

Ott, M., Robertson, J.D., Gogvadze, V., Zhivotovsky, B., Orrenius, S., 2002: Cytochrome c release from mitochondria proceeds by a two-step process. Proceedings of the National Academy of Sciences 99, 1259–1263.

Palm, D., Streit, D., Shanmugam, T., Weis, B.L., Ruprecht, M., Simm, S., Schleiff, E., 2019: Plant-specific ribosome biogenesis factors in *Arabidopsis thaliana* with essential function in rRNA processing. Nucleic Acids Research 47, 1880–1895.

Park, C.S., Hwang, E.K., 2014: Isolation and evaluation of a strain of *Pyropia yezoensis* (Bangiales, Rhodophyta) resistant to red rot disease. Journal of Applied Phycology 2, 811–817.

Park, C.S., Kakinuma, M., Amano, H., 2006: Forecasting infections of the red rot disease on *Porphyra yezoensis* Ueda (Rhodophyta) cultivation farms. Journal of Applied Phycology 18, 295–299.

Patro, R., Duggal, G., Love, M.I., Irizarry, R.A., Kingsford, C., 2017: Salmon provides fast and bias-aware quantification of transcript expression. Nature Methods 14, 417.

Perier, C., Tieu, K., Guégan, C., Caspersen, C., Jackson-Lewis, V., Carelli, V., Martinuzzi, A., Hirano, M., Przedborski, S., Vila, M., 2005: Complex I deficiency primes Bax-dependent neuronal apoptosis through mitochondrial oxidative damage. Proceedings of the National Academy of Sciences 102, 19126–19131.

Poljsak, B., Šuput, D., Milisav, I., 2013: Achieving the balance between ROS and antioxidants: when to use the synthetic antioxidants. Oxidative Medicine and Cellular Longevity, 956792.

Provasoli, L., 1963: Organic regulation of phytoplankton fertility. The Sea 2, 165–219.

Pruitt, K.D., Tatusova, T., Maglott, D.R., 2005: NCBI Reference Sequence (RefSeq): a curated non-redundant sequence database of genomes, transcripts and proteins. Nucleic Acids Research 33, D501–D504.

Rabeta, M., Faraniza, R.N., 2013: Total phenolic content and ferric reducing antioxidant power of the leaves and fruits of *Garcinia atrovirdis* and *Cynometra cauliflora*. International Food Research Journal 20, 1691–1696.

Reape, T.J., Molony, E.M., McCabe, P.F., 2008: Programmed cell death in plants: distinguishing between different modes. Journal of Experimental Botany 59, 435–444.

Sampath-Wiley, P., Neefus, C.D., 2007: An improved method for estimating R-phycoerythrin and R-phycocyanin contents from crude aqueous extracts of *Porphyra* (Bangiales, Rhodophyta). Journal of Applied Phycology 19, 123–129.

Santos-Sánchez, N.F., Salas-Coronado, R., Hernández-Carlos, B., Villanueva-Cañongo, C., 2019: Shikimic acid pathway in biosynthesis of phenolic compounds. In: Soto-Hernández, M. (ed.), Plant Physiological Aspects of Phenolic Compounds, IntechOpen, London.

Sonnhammer, E.L., Eddy, S.R., Durbin, R., 1997: Pfam: a comprehensive database of protein domain families based on seed alignments. Proteins: Structure, Function, and Bioinformatics 28, 405–420.

Takagi, H., Watanabe, S., Tanaka, S., Matsuura, T., Mori, I. C., Hirayama, T., Shimada, H., Sakamoto, A., 2018: Disruption of ureide degradation affects plant growth and development during and after transition from vegetative to reproductive stages. BMC Plant Biology 18, 287.

Untergasser, A., Cutcutache, I., Koressaar, T., Ye, J., Faircloth, B.C., Remm, M., Rozen S.G., 2012: Primer3 - new capabilities and interfaces. Nucleic Acids Research 40, e115–e115.

Van Loo, E.J., Hoefkens, C., Verbeke, W., 2017: Healthy, sustainable and plant-based eating: Perceived (mis) match and involvement-based consumer segments as targets for future policy. Food Policy 69, 46–57.

Vanlerberghe, G.C., 2013: Alternative oxidase: a mitochondrial respiratory pathway to maintain metabolic and signaling homeostasis during abiotic and biotic stress in plants. International Journal of Molecular Sciences 14, 6805–6847.

Vianello, A. Zancani, M., Peresson, C., Petrussa, E., Casolo, V., Krajňáková, J., Patui, S., Braidot, E., Macrì, F., 2007: Plant mitochondrial pathway leading to programmed cell death. Physiologia Plantarum 1, 242–252.

Virolainen, E., Blokhina, O., Fagerstedt, K., 2002: Ca2+-induced high amplitude swelling and cytochrome c release from wheat (*Triticum aestivum* L.) mitochondria under anoxic stress. Annals of Botany 4, 509–516.

Wang, L., Mao, Y., Kong, F., Li, G., Ma, F., Zhang, B., Sun, P., Bi, G., Zhang, F., Xue, H., 2013: Complete sequence and analysis of plastid genomes of two economically important red algae: *Pyropia haitanensis* and *Pyropia yezoensis*. PLoS One 8, e65902.

Waterhouse, R.M., Seppey, M., Simão, F.A., Manni, M., Ioannidis, P., Klioutchnikov, G., Kriventseva, E.V., Zdobnov, E.M., 2018: BUSCO applications from quality assessments to gene prediction and phylogenomics. Molecular Biology and Evolution 35, 543–548.

Werner, A.K., Witte, C.P., 2011: The biochemistry of nitrogen mobilization: purine ring catabolism. Trends in Plant Science 16, 381–387.

Werner, A.K., Medina-Escobar, N., Zulawski, M., Sparkes, I.A., Cao, F.Q., Witte, C.P., 2013: The ureide-degrading reactions of purine ring catabolism employ three amidohydrolases and one aminohydrolase in Arabidopsis, soybean, and rice. Plant Physiology 163, 672–681.

Westphal, D., Dewson, G., Czabotar, P.E., Kluck, R.M., 2011: Molecular biology of Bax and Bak activation and action. Biochimica et Biophysica Acta 1813, 521–531.

Ye, J., Zhang, Y., Cui, H., Liu, J., Wu, Y., Cheng, Y., Xu, H., Huang, X., Li, S., Zhou, A., 2018: WEGO 2.0: a web tool for analyzing and plotting GO annotations, 2018 update. Nucleic Acids Research 46, W71–W75.

Zayadan, B., Purton, S., Sadvakasova, A., Userbaeva, A., Bolatkhan, K., 2014: Isolation, mutagenesis, and optimization of cultivation conditions of microalgal strains for biodiesel production. Russian Journal of Plant Physiology 1, 124–130.

Zhang, T., Li, J., Ma, F., Lu, Q., Shen, Z., Zhu, J., 2014: Study of photosynthetic characteristics of the *Pyropia yezoensis* thallus during the cultivation process. Journal of Applied Phycology 2, 859–865.